



Optimal droplet transfer mode maintenance for wire + arc additive manufacturing (WAAM) based on deep learning

Jian Qin¹ · Yipeng Wang² · Jialuo Ding¹ · Stewart Williams¹

Received: 14 February 2022 / Accepted: 28 June 2022 / Published online: 24 July 2022
© The Author(s) 2022

Abstract

In the last decade, wire + arc additive manufacturing (WAAM), which is one of the most promising metal additive manufacturing technologies, has been attracting high interest from both academia and industry. WAAM systems are increasingly employed in the industry and academia, but there are still several challenges and barriers to process stability control. The process stability is highly dependent on how the molten feed wire is added into the melt pool, which is known as the droplet transfer mode. To ensure a stable WAAM deposition process, it is essential to maintain the transfer mode in a suitable stable status. Without an effective transfer mode control method, the operators need to determine and control the transfer mode based on their experience using manual adjustment, which is difficult to achieve in a long period of production process. In this paper, a deep learning-based technology was proposed for the control of the droplet transfer mode based on the data collected from the WAAM process. A long short term memory neural network was applied as the core transfer mode classification model. A time-series data, arc voltage, was collected and statistical and frequency features were extracted, which included 11 relevant features, as the inputs of the classification model. Then, the distance between the melted wire and the melt pool was adjusted based on the determined transfer mode to keep a suitable stability of the process. A case study was used to evaluate the proposed approach and to show its merit. The proposed approach was compared to three commonly used machine learning algorithms, *k*-nearest neighbours, support vector machine, and decision tree. The proposed method obtained the highest accuracy in determining the transfer mode, which was over 91%. The performance of the proposed approach was also evaluated by the single-pass and oscillated wall building. The proposed deep learning based approach improved the process stability in real-time, which resulted in better deposition qualities, in terms of geometry size and processing cleanliness compared to without control. Furthermore, this data-driven method could be applied to other WAAM processes and materials.

Keywords WAAM · Deposition process stability · Droplet transfer mode · Deep learning

Introduction

As one of the processes of direct energy deposition (DED), WAAM has significant advantages for producing large metal components, such as the unconstrained volume of building parts, less material waste, and short time to market (Wu et al., 2018). It has become one of the most promising alternatives to produce large metal components at a high deposition rate

(Williams et al., 2016). Compared with other AM processes, such as the laser powder bed process, WAAM can provide a higher deposition rate for large scale metal part production in an environmental-friendly condition (Cunningham et al., 2018; Khanna et al., 2021). However, it is challenging to maintain and control a stable deposition process for many reasons, such as unpredictable droplet transfer caused by thermal mass variation, which can significantly affect the deposition geometry, especially the layer height (Shi et al., 2021). To describe the process of material droplet feeding in the melt pool, four droplet transfer modes were defined, namely permanent contact mode (TM1), intermittent mode (TM2), fleeting mode (TM3), and non-contact mode (TM4) (Ríos et al., 2019).

These four modes are classified based on the duration of droplet formation and the time of contact between droplet

✉ Yipeng Wang
wyp092@163.com

¹ Welding Engineering and Laser Processing Centre, Cranfield University, Conway house, University Way, Cranfield MK40 3AA, UK

² Institute of Light Alloy and Processing, Faculty of Materials and Manufacturing, Beijing University of Technology, Beijing 100124, China

and melt pool. When the wire is permanently contacted in the melt pool, this type of droplet transfer is defined as TM1, the permanent contact transfer mode. In the intermittent transfer mode (TM2), the time for droplet formation is equal to the duration of contact. In the fleeting transfer mode (TM3), the droplet growth time is much longer than the contact time. The transfer mode is defined as ‘non-contact’ (TM4) when the contact is entirely lost and the droplet transfers by free flight. Having a suitable stable transfer mode significantly improves the process stability, TM2 has been shown to be the optimal droplet transfer mode for WAAM (Ríos et al., 2019). To keep the process stable, the transfer mode must be dynamically detected and controlled in real-time. The wire feeding position is the most critical parameter for controlling transfer mode and process stability (Wang et al., 2021a). Generally, operators tend to manually modify the wire position with the live images taken from the process camera and electrical wire-positioning to maintain a stable transfer mode. This is done based on their knowledge and experience of deposition conditions. However, it is challenging and expensive for operators to continuously maintain the optimum wire position throughout the process, which may take many days. To overcome this challenge, online process monitoring and closed-loop control of WAAM processes would be a good solution (Xia et al., 2020). Critical is the effective identification of droplet transfer mode for constructing a control system. Due to the short response time required, it is difficult to identify the transfer mode by the droplet formation time and contact time. Therefore, it is necessary to find a method of identifying the transfer mode. It has been found that when a droplet falls from the end of the wire to the melt pool, or the wire touches the melt pool it causes a sudden change in the voltage between the end of the wire and the melt pool (Yudodibroto et al., 2004). Therefore, the arc voltage related signals can be used as an efficient medium to identify the droplet transfer mode.

Imanaga et al., (2000) reported research about monitoring arc voltage to identify the transfer mode in the gas tungsten arc (GTA) welding process. An extra DC power supply was used in their study, to support the constant current between the end of the filler wire and the substrate. When droplets contacted the melt pool, the voltage of the extra DC showed a sudden drop. By determining the average frequency of the sudden change in a certain period, the transfer mode can be identified. In their experiment, when the frequency was low, the process was in TM1 or TM3. In the TM2 this frequency was shown in a high value. They also indicated the impact factors of the process to influence the transfer mode, in terms of wire feed speed, current, gas flow rate, and the distance between the end of the filler wire and the melt pool. The first three factors were decided by the processing requirement, meaning that it was not possible to change them during deposition. Therefore, the distance between the end of filler wire

and melt pool was considered one of the available control targets in their research. Ríos et al., (2019) also focused on arc voltage measurement and wire position control to keep the WAAM process stable. In their research, the simple moving averages (SMA) of the arc voltage were used to indicate the sudden changes in the arc voltage without any extra devices. In this research, different transfer modes caused a different number of arc voltage sudden changes. These sudden changes proved to be able to determine the contact frequency (CF) which determines the number of droplets contacting the melt pool per unit of time. The contact frequency of TM1 was 0 and TM3 was generally larger than TM2. The paper also explained that the wire position is an important factor for transfer mode. However, this study did not establish a correlation between the wire position, arc monitoring signal and the transfer mode. The droplet transfer mode classification can also be used in wire based laser AM systems based on arc voltage. Hagqvist et al., (2015) published a method to determine the transfer mode of a laser-based DED AM process by monitoring the resistance between the end-effector and workpiece, which was calculated by arc voltage and current. Then, a mathematical model was built for calculating the actual distance to compare with the required distance. In the next stage of the research, iterative learning control was proposed based on this relationship (Hagqvist et al., 2014). By using the proposed control strategy, the height of the wall that was deposited was more stable and smoother than the uncontrolled one. The importance of wire position for transfer mode was also observed by Miranda et al., (2008); Dilthey et al., (1995); Sorensen and Eagar, (1990). However, the solution to this issue is still not clear and requires a deeper investigation of the relevant factors.

Current research commonly focuses on a specific system and material, and the algorithms developed are specific to this arrangement. It is hard to apply these algorithms to other WAAM systems with different power sources and different filler materials. Meanwhile, current research on droplet transfer mode identification is still too vague to build an accurate and generic model for WAAM systems. To overcome these challenges, deep learning is considered as a solution which is entirely driven by data (Qin et al., 2022). It makes the methodology more generic and easier to be applied to different WAAM systems. Although deep learning has not been used and studied in any relevant research, it has been applied in WAAM related research since the 1990s (Andersen et al., 1990). Artificial neural network (ANN) modelling was used in Andersen et al. (1990) research to predict the key features of the arc welding process based on empirical data. In their study, four process related features were considered as the input of the ANN model, such as arc current, voltage, travel speed, wire feed speed, to predict four key performance targets of the arc welding process, such as bead width, penetration, reinforcement height, and cross-section area. Due

to the difficulty of collecting data from arc welding, only 42 data points were used to train and test the ANN model. However, even with the limited dataset size, the results were acceptable.

Different to the studies of geometry prediction, the relationship between transfer mode and arc voltage is more time related. According to the attribute and definition of time-series data (Fu, 2011), arc voltage is typical time-series data which is indexed in order of time (Riza Alvy Syafi'i et al., 2018). This type of data is generally not independent, which means each data point has a strong relation to others in the time dimension (Raubitzek & Neubauer, 2021). One of the deep learning technologies, the long short term memory neural network (LSTM-NN), was designed to process the time-series data (Sherstinsky, 2020). LSTM is a special type of recurrent neural network (RNN), which is usually used for processing time-series data such as data of audio (Marchi et al., 2014), video (Yue-Hei Ng et al., 2015), and text (Abandah et al., 2015). This type of neural network is designed for recording information for a long period. One example in AM relevant research is the fused deposition AM process to process the acoustic data (Marchi et al., 2014). In this study, LSTM-NN was applied to identify six process action features including defect classes. The classification accuracy rate was as high as 96.96% which provided an opportunity to repair the defects. This method has a huge potential to be applied for

the droplet transfer mode classification in WAAM. However, there are no relevant research reported so far.

This paper innovatively applies LSTM-NN based deep learning technology to the classification of droplet transfer mode for WAAM process stability maintenance. The droplet transfer mode is firstly modelled and classified by a LSTM-NN based deep learning model. Then, wire position control is used to dynamically maintain the droplet transfer mode in optimal conditions for a stable deposition process. The proposed approach is introduced as a framework, which includes the stage of data pre-process and feature extraction, LSTM-NN based transfer mode classification and transfer mode controlling. A case study is presented to evaluate the performance of the proposed method, in which the produced parts were compared.

Methodology

Deep learning based framework for WAAM process stability maintenance

The proposed framework of the process stability includes three stages, data pre-processing and feature engineering stage, transfer mode classification stage, and transfer mode maintenance stage. The framework is shown in Fig. 1.

After sensing and collecting raw arc voltage data, the raw data is tapered into multiple windows. Two types of features

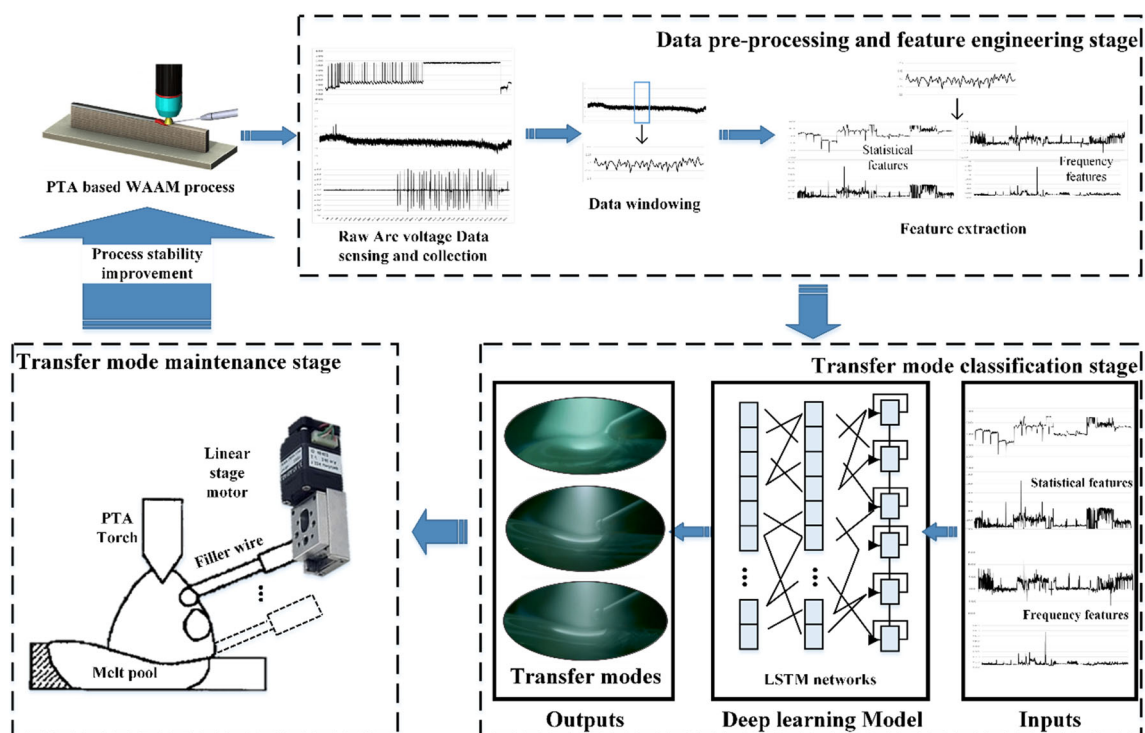


Fig. 1 Deep learning based framework for WAAM process control

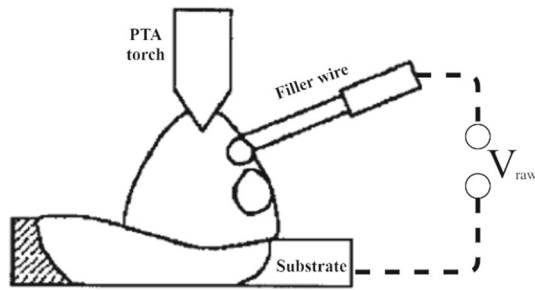


Fig. 2 Arc voltage acquisition

are extracted from this time-series data for each data window, statistical features, and frequency features. These features are the inputs of the LSTM-NN, in which the droplet transfer mode is the target. Based on the LSTM-NN modelling, the transfer mode is identified.

Data pre-process and feature extraction

During the process, raw arc voltage data is continually collected from the power source, which is typical time-series data. To discover the relevant patterns to the transfer modes, this time-series data is firstly tapered into several rectangular windows of equal size. The windowing process is donated as:

$$V_{raw} = [v_1, v_2, v_3, \dots, v_N] \quad (1)$$

$$V_T = [[v_1, v_2, \dots, v_t], [v_{t+1}, v_{t+2}, \dots, v_{2t}], \dots, [v_{(n-1)t+1}, v_{(n-1)t+2}, \dots, v_{nt}]] \quad (2)$$

$$N = (n * t) + a \quad (3)$$

where V_{raw} is the collected raw arc voltage dataset, which measures the voltage between supply wire and substrate shown in Fig. 2. V_{raw} consists of the number of N voltage data points.

V_T is represented as the windowing arc voltage dataset which includes n data windows and each data window has t voltage data points. Each time window data is denoted as V_t . There are several voltage data points dropped by the windowing process which is from v_{nt} to v_N . In this study, two types of features were extracted from the windowed arc voltage datasets, the statistical feature, and the frequency feature. For each time window dataset, these two types of features are extracted. For example, the extremum values, variance, and mean values can be statistical features, and spectral skewness and spectral kurtosis can be frequency features.

Table 1 Droplet transfer mode definition

Inputs:	t_c : Contacting time between droplet and melt pool t_f : Formation time of droplet
Results:	TM: Transfer mode
1: Function	$TransferMode(t_c, t_f)$
2:	If $t_c > t_f$ then
3:	TM = Transfer mode 1 (TM1)
4:	Else if $t_c = t_f$ then
5:	TM = Transfer mode 2 (TM2)
6:	Else if $t_c < t_f$ then
7:	TM = Transfer mode 3 (TM3)
8:	Else if $t_c == 0$ then
9:	TM = Transfer mode 4 (TM4)
10:	End if
11:	return result
12:	end function

LSTM-NN based droplet transfer mode classification

As the output feature of the LSTM-NN model, the historical droplet transfer mode of each processing period is defined by Table 1 (Ríos et al., 2019) shown below. The mathematical operators follow the pseudocode (Oda et al., 2015). The droplet transfer mode is defined by the comparison of two periods of time, which are the contacting time between the droplet and the melt pool, and the formation time of the droplet. As shown in the video image sequence for a complete droplet transfer cycle (Fig. 3), the period of droplet formation and its growth before contacting the melt pool is defined as t_f , and t_c represents the duration time of contacting between the droplet and melt pool until the droplet detaches from the end of wire. The time is determined by a process camera.

By applying the inputs of statistical and frequency features shown as the proposed framework, the LSTM is then used for modelling the transfer mode of the WAAM process. Different from other RNN structures, an LSTM cell typically includes three gates forgotten gate, the input gate, and the output gate for remembering the information, as shown in Fig. 4.

In the LSTM structure, C is called the cell state which is for transferring the information. Under the effect of forgetting, the input gate, the LSTM cell can remove or add information. The forget gate is denoted as:

$$f_t = \sigma(W_f(g_{t-1}, V_T) + b_f) \quad (4)$$

where σ is the sigmoid function. W_f is the cell weight. g_{t-1} is the output from the last layer, and b_f is the bias. The input gate is also used for storing the new information. It is combined into two sections, one is a sigmoid section, which

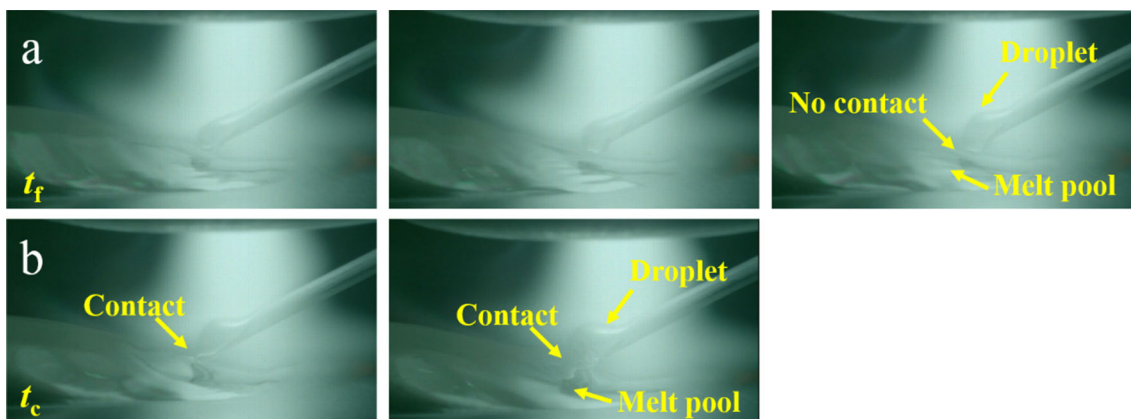


Fig. 3 Two periods of droplet transfer process: a Duration time of droplet formation t_f ; b Contacting time between droplet and melt pool t_c

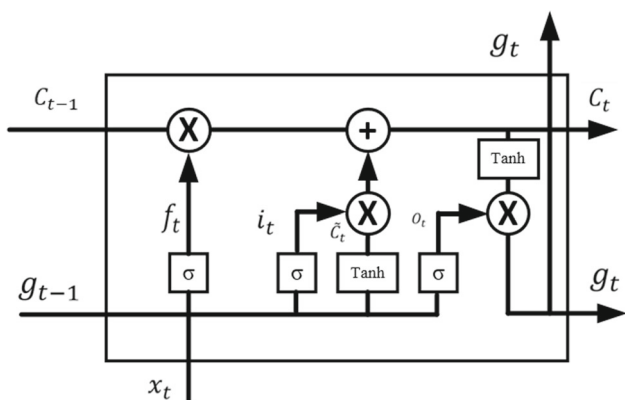


Fig. 4 Structure of LSTM cell

is used for deciding the updated value:

$$i_t = \sigma(W_i(g_{t-1}, V_T) + b_i) \tag{5}$$

The second section is a vector of new candidate values (\tilde{C}_t) that can be added to the state:

$$\tilde{C}_t = \tanh(W_C(g_{t-1}, V_T) + b_c) \tag{6}$$

By considering the forget and input gate, the new cell state is shown as:

$$C_t = f_t * C_{t-1} + i_t * \tilde{C}_t. \tag{7}$$

Finally, the output gate is denoted as:

$$O_t = \sigma(W_o(g_{t-1}, x_t) + b_o), \tag{8}$$

The output for the next layer is:

$$g_t = O_t * \tanh(C_t). \tag{9}$$

The two Eqs. (8 and 9) are used to generate the output of the cell, which are also the inputs of the next cell. Other parameters of LSTM and the full connection neural network are set individually, such as the size of the network, optimiser, loss function, and learning rate, etc. These parameters are dependent on the specific case, which is introduced in the case study.

Transfer mode maintenance stage

Based on the classification decided by the droplet transfer mode modelling stage, when the transfer mode is TM1, which means the wire is too low to keep the process stable, the wire is gradually moved vertically up until the transfer mode switches to TM2. If the transfer mode is TM2, the wire position remains the same. If the transfer mode is TM3 or TM4, which means the wire is too high to keep the process stable, the wire is moved vertically down depending on the current processing situation.

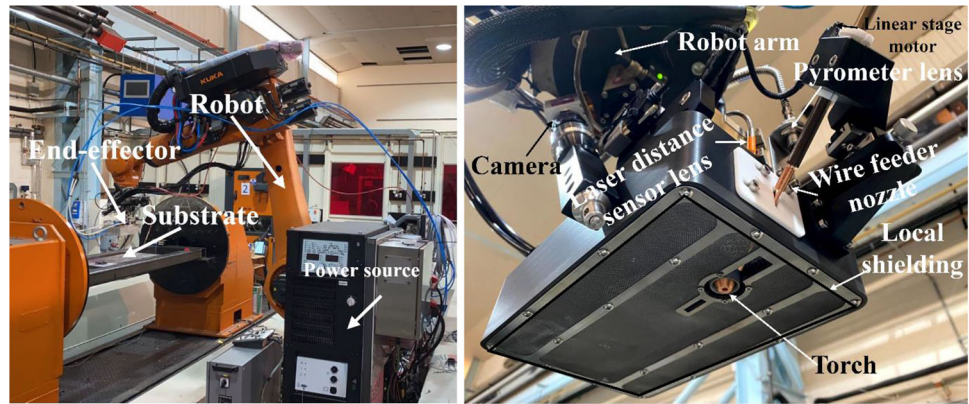
Case study

To reveal the performance of the proposed approach for maintaining the WAAM deposition process stability, a case study was designed and performed. In this case study, two different Ti-6Al-4 V walls were built by using the proposed approach. The results are compared to the ones that were built without using the proposed approach.

WAAM system setup

The experimental system is a robotic plasma transferred arc (PTA) WAAM system consisting of a power source, a wire feeder, an industrial robot, an inert gas local shielding system (Ding et al., 2015), a data acquisition system, and an electrical wire position fine adjustment system. The WAAM system is

Fig. 5 Robotic based WAAM system and end effector



shown in Fig. 5. In this system, the PTA power source was the EWM Tetrix 352 Plasma machine, A KUKA industrial robot was used to provide the movement of the tool relative to the building substrate. The filler wire was Ti-6Al-4V, and its diameter was 1.2 mm.

The entire case study was implemented in an argon filled environment which was provided by a local shielding system built in an end-effector that was mounted on the robot arm. This end-effector was composed of an arc vision camera, a torch, a wire feed nozzle, a linear stage motor, a lens of the pyrometer and a laser distance sensor, which is also shown in Fig. 5. The linear stage motor was connected to the wire feed contact tip for fine-tuning the wire position in the vertical direction. This motor has a travel range of 10 mm at a speed of up to 14 mm/s and the minimum movement step is 0.01 mm. Two different geometries were built in the case study. The first one is a single-pass wall, while the other one is an oscillated wall. The process parameters used for building these two walls are shown in Table 2, these were determined according to the plasma arc additive manufacturing process investigation of Ti-6Al-4V (Martina et al., 2012). During deposition, the wire feed speed remained unchanged, and the droplet transfer mode was controlled by adjusting the distance between end of the melting wire and the molten pool through the wire position fine-turn system.

Data acquisition and processing

The arc voltage was captured by a National Instruments (NI) device (NI USB-6009) with a sampling rate of 1000 Hz. To extract the features from the raw voltage data, the raw signals were averaged and processed by a Butterworth low-pass filter with zero-phase and second-order under a cut-off frequency of 80 Hz to remove the high frequency variations in the raw signal. Then two types of features were extracted, and the details of each type of the feature are shown in Table 3. A total of 11 features were extracted from the raw arc voltage data, of which 7 are statistical features and 4 are frequency features (Desai et al., 2013). By extracting these features,

each windowed time-series dataset is transferred as a dataset of a 11-feature dataset.

The final step of data pre-processing is normalisation to avoid data redundancy and balance the importance of each feature. This normalised pre-processed dataset is the main input for transfer model modelling. To generate the dataset of this case study, more than 350,000 data points were collected from 23 layers of deposition. The proportion of each transfer mode (TM1, TM2, TM3, and TM4) was about 28.05%, 50.17%, 18.96 and 2.82% respectively.

Experimental results

The results of this case study focused on validating the proposed method, in terms of the accuracy of the transfer mode classification and the performance of process stability maintenance. Firstly, the classification accuracy of the LSTM-NN is compared with three benchmark machine learning algorithms. Then, the part which was built under the proposed stability maintenance method is compared to the one that was built without using the method.

Results of droplet transfer mode classification

Before introducing the results of transfer mode classification, it is interesting to realise the correlations between the input features and the transfer mode. Table 4 illustrates the Pearson correlation coefficient ($\rho_{X,Y}$), shown in the following equation, which is a typical numerical measure of the strength of the relationship between two features. In this equation, $Cov(X, Y)$ is the covariance between two features, σ_X is the standard deviation of one feature and σ_Y is the standard deviation of another feature. The value of this coefficient is between -1 to $+1$, where ± 1 represents the strongest linear relationship, and 0 indicates the weakest relationship (Asuero et al., 2006). In general, when the correlation coefficient is between $+0.3$ and -0.3 , the two feature has a weak relationship. When this coefficient is between $+0.3$ and $+0.8$ or

Table 2 Process parameter setup

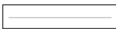

	Path trajectory	Travel speed	Current	Wire feed speed	Plasma gas flowrate	Shielding gas flowrate	Wire feed angle	Nozzle to substrate stand-off
Single-pass wall		4.1 mm/s	175 A	2.1 m/min	0.8 l/min	8.0 l/min	25°	8 mm
Oscillated wall		5.5 mm/s	194 A	2.5 m/min				

Table 3 List of extracted features

Feature type	Feature name	Equation
Statistical	Root mean square (e_{rms})	$\sqrt{\frac{1}{T} \text{Sum}(V_T^2)}$
	Variance (σ^2)	$\frac{1}{T} \text{Sum}(V_T - \bar{V}_T)$
	Maximum (max)	$\text{Max}(V_T)$
	Minimum (min)	$\text{Min}(V_T)$
	Skewness (skp)	$E\left[\left(\frac{V_T - \mu}{\sigma}\right)^3\right]$
	Kurtosis (β_2)	$E\left[\left(\frac{V_T - \mu}{\sigma}\right)^4\right]$
	Peak to peak (d_{ptp})	$\text{Max}(V_T) - \text{Min}(V_T)$
Frequency	Spectral Skewness (skp_s)	$\text{sum}\left(\left(\frac{v_i^i - \bar{V}_T}{\sigma}\right)^3\right) S(V_T^i)$
	Spectral Kurtosis (β_{2_s})	$\text{sum}\left(\left(\frac{v_i^i - \bar{V}_T}{\sigma}\right)^4\right) S(V_T^i)$
	Number of negative peaks (P_{neg})	Count(if : $v_i^i > V$ (when v_i is positive))
	Number of positive peaks (P_{pos})	Count(if : $v_i^i < -V$ (when v_i is negative))

* v_i^i is the data filtered by the low-pass filter

Table 4 Correlation coefficient of input features and droplet transfer mode

Features	e_{rms}	σ^2	max	min	skp	β_2	d_{ptp}	skp_s	β_{2_s}	P_{neg}	P_{pos}
TM	0.55	0.57	0.48	0.75	0.71	0.16	0.49	0.4	0.52	0.64	0.56

– 0.8 and – 0.3, the indicated features are reasonably correlated. When it is larger than + 0.8 or less than – 0.8, there is a strong correlation between the two features (Charaniya et al., 2010).

$$p_{X,Y} = \frac{Cov(X, Y)}{\sigma_X \sigma_Y} \tag{10}$$

From the above correlation table, the skewness value, minimum value and the negative peak number are the top three relevant features of the transfer mode, which correlation coefficients are 0.69, 0.66 and 0.65, respectively. But even for the lowest correlation coefficient of the features, kurtosis, this value is still 0.3 which shows a reasonable correlation to the transfer mode. Comparing between two feature

types, statistical and frequency features, the average correlation coefficient of statistical features, including root mean square, variance, maximum and minimum values, skewness, kurtosis and value between peak and peak, is 0.51, which is slightly higher than the average correlation coefficient, 0.48 of frequency features, including spectral skewness, spectral kurtosis, and the number of negative and positive peaks.

In this paper, three conventional ML algorithms are compared to the proposed LSTM-NN, which are k -nearest neighbours (k -NN), support vector machine (SVM), and decision tree (DT) (Bonaccorso, 2017). All algorithms were implemented by Python within Scikit learning (Pedregosa et al., 2011) and Keras (Gulli & Pal, 2017) library. The LSTM-NN in this case study includes four layers, one LSTM

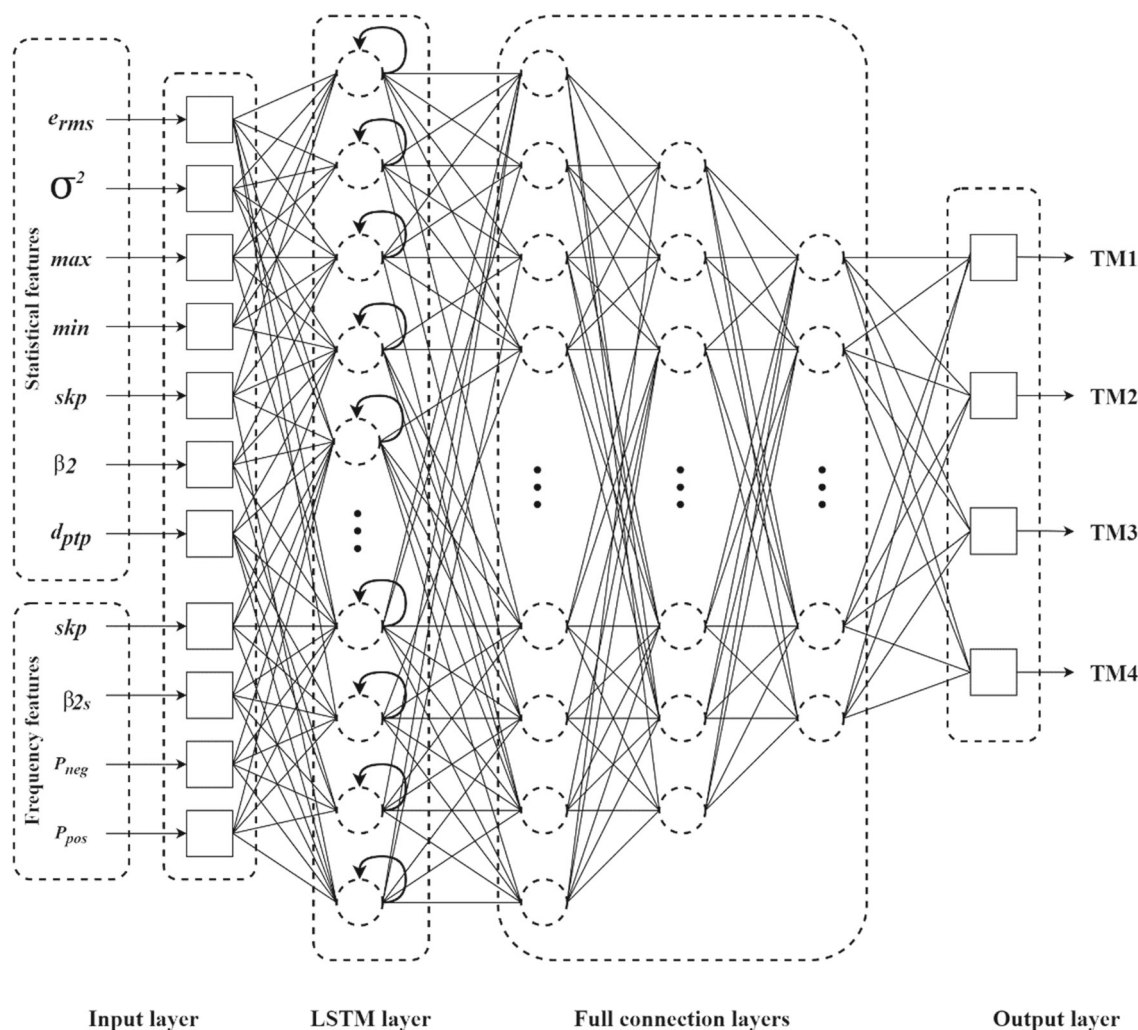


Fig. 6 Structure of LSTM-NN

layer, and three full connection layers. There were 100, 50, 30 neurons in each full connection layer respectively, as shown in Fig. 6. Furthermore, the optimiser was Adam, loss function was categorical cross entropy, and learning rate was 0.1 in the proposed neural network (Gulli & Pal, 2017). Five-fold cross-validation was adopted as it is one of the most used evaluation methods for ML algorithms (Wiens et al., 2008). The accuracy ratio was used as the main evaluation metric for this multiclass classification problem, which is denoted as following equation (Hossin & Sulaiman, 2015).

$$\text{Accuracy ratio} = \frac{TP + TN}{TP + TN + FP + FN}, \quad (11)$$

The evaluation result comparison is shown in Table 5. The accuracy ratio in the table represents the percentage of corrected classification. Overall, all machine learning algorithms have obtained over 0.8 of the accuracy ratios.

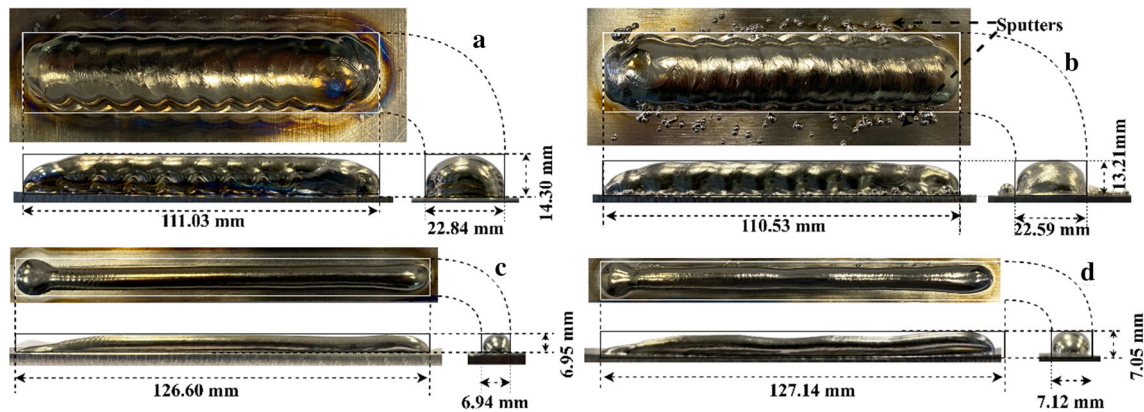
What stands out in the table is that the proposed LSTM-NN obtained the highest accuracy ratio which is 0.911 on average for single-pass walls and Oscillated walls. Overall, these classification accuracy ratios indicate that the proposed LSTM-NN can determine the transfer mode most accurately comparing to the other conventional ML algorithms.

Performance of process stability maintenance

Figure 7 compares the geometries of the parts that were produced with and without the proposed process stability maintenance approach. The dimensional data of 3 directions of the deposited structures are presented, these are the top, front and left directions, as shown in Fig. 7. There were 8 layers of the oscillated wall and 4 layers of the single-pass wall. Comparing Fig. 7a and b, the parts without process stability maintenance generated a high level of spattering, while the parts built with the proposed approach were clean. Spattering during the deposition process may affect the arc stability

Table 5 Droplet transfer mode classification mode comparison

Algorithm	<i>k</i> -NN		SVM		DT		LSTM-NN	
	Single-pass wall	Oscillated wall	Single-pass wall	Oscillated wall	Single-pass wall	Oscillated wall	Single-pass wall	Oscillated wall
Accuracy ratio	0.878	0.872	0.840	0.848	0.857	0.879	0.904	0.918

**Fig. 7** **a** Oscillated wall with process stability maintenance; **b** oscillated wall without process stability maintenance; **c** single-pass wall with process stability maintenance; **d** single-pass wall without process stability maintenance

and reduce the protective effect of the shielding gas, thereby resulting in a poor bead formation. It may also cause material waste and uniformity of the layer height which should be avoided for the WAAM process. The main reason for the improvement with droplet transfer control system is that this maintained the droplet transfer mode in TM2, and significantly reduced TM3. While the process without using the control system experienced a large amount of time in TM3. In TM2, due to the surface tension of the liquid metal, the droplet transfers to the melt pool with a liquid bridge, for example, the droplet is simultaneously in contact with the melting wire and melt pool on the substrate. In TM3, the droplet is formed at a high position and the lateral arc force pushes the droplet away from the melt pool, thus forming spatters.

Additionally, as shown in Fig. 7c and d, the surface waviness and the variation of layer height and width of the part built by the proposed approach are lower than the part without the approach. Further statistical comparison of the height and width are presented in Table 6.

The values of this table were measured from the finished part. Each perspective includes more than 20 measurements. To avoid the influence of edge sinking, the measurements were taken focusing on the middle section of the parts. Especially for the single-pass wall, the standard deviation of each dimension is much smaller than the one without the droplet transfer control system (about 4 times lower in height dimension, 5 times in width dimension) which indicates that this method can significantly improve the uniformity of the bead

geometry. On average, the oscillated wall without the proposed approach has the greatest standard deviation of layer height and width, respectively 0.55 mm, and 0.70 mm.

To achieve a stable process, the wire position was fine-tuned. Figure 8 shows how the wire position changed between different modes in the single-pass wall process. Figure 8a shows that the transfer mode changed from TM1 to TM 2, and Fig. 8b shows the transfer mode changed from TM3 to TM2. The response time of the process is relatively short taking only about one second from detecting the transfer mode to changing the wire position to maintain a stable deposition position. The TM4 mode did not appear in the wall building as the initial wire position was in a reasonable position.

In the control system the stage motor moved the wire position vertically and kept the transfer mode of the deposition in TM2 when the LSTM-NN identified the transfer mode was not the TM2. Since the transfer mode became stable (TM2), the wire position remained in a reasonable range to maintain the status.

Discussion

From the comparison of the parts built with and without droplet transfer control, it is clear that the droplet transfer mode was kept in an optimal one, thereby maintaining a stable deposition process. The results of the case study broadly support the work of other studies in this area link-

Table 6 Statistical analysis of the dimension measurement

Dimension measurements	With the droplet transfer control system		Without droplet transfer control system	
	Height	Width	Height	Width
Oscillated wall				
Maximum (mm)	14.67	23.89	13.69	23.83
Minimum (mm)	13.47	22.04	11.94	21.63
Mean (mm)	14.30	22.84	13.21	22.59
Standard deviation (mm)	0.34	0.58	0.55	0.70
Single-pass wall				
Maximum (mm)	7.10	7.16	7.71	7.84
Minimum (mm)	6.81	6.80	6.50	6.85
Mean (mm)	6.95	6.94	7.05	7.34
Standard deviation (mm)	0.09	0.11	0.43	0.41

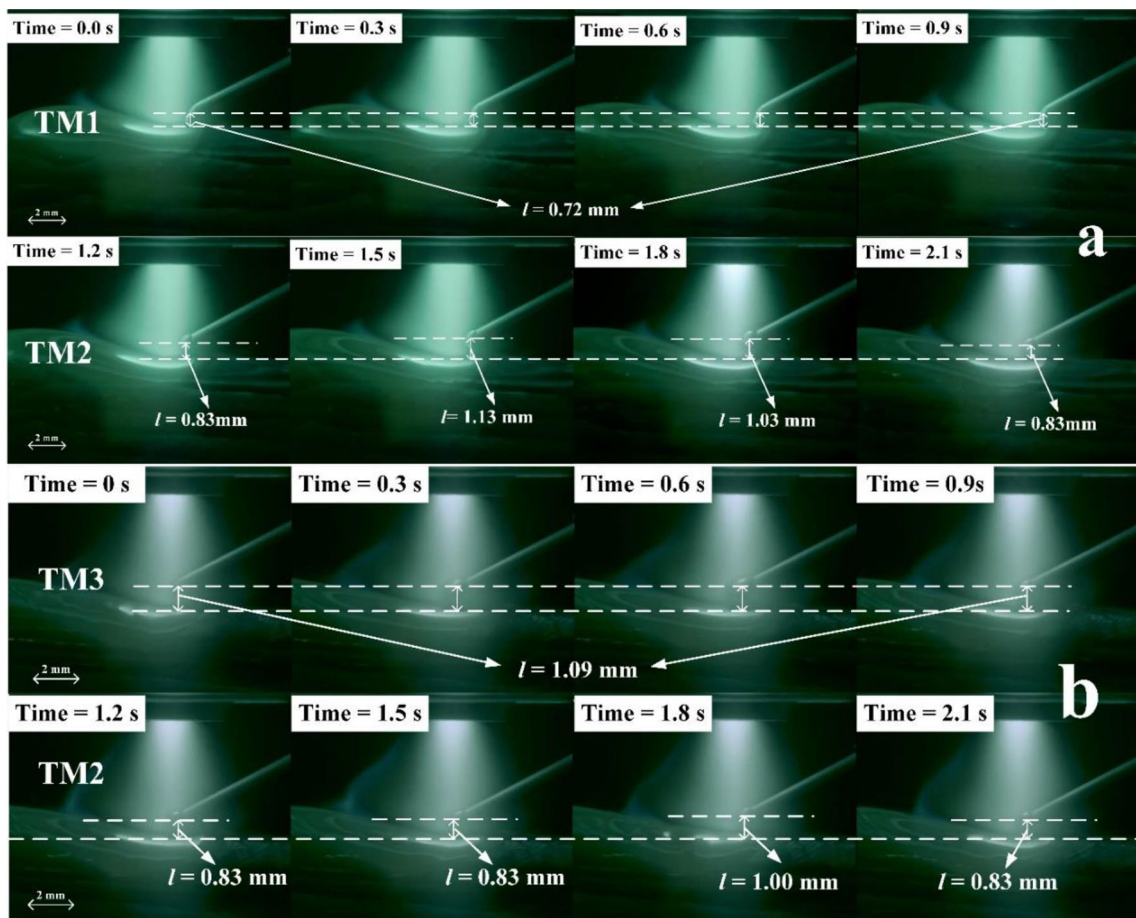


Fig. 8 a Wire position fine-tune for changing transfer mode from TM1 to TM2; b Wire position fine-tune for changing transfer mode from TM3 to TM2

ing droplet transfer mode and process stability. By building two different shapes of walls, the single-pass and oscillated walls that have a lower waviness of surface and variation of layer height and width, the control system increases the effective area of the parts, which also reduces the materials used. In the case study, two shapes of walls were built using different process parameters and the control system results were similar. The variability of process parameters has been considered when extracting the relevant features from arc voltage. Two different sets of process parameters were used to test the control system with very different operating parameters which caused different processing conditions and thermal conditions. This meant that the optimal wire position was also different (Wang et al., 2021a, 2021b). However, it was demonstrated that the proposed droplet transfer control system was able to find the optimum position even though these were different. The processing and physical investigation related studies of wire position in WAAM processes is not the main aim of this research (Ríos et al., 2019). But it needs further study to understand the physical knowledge of the process.

Additionally, the case study results reflect those of Ríos et al., (2019) who also found that the TM2 is recommended for the WAAM deposition process. TM1 can cause stabbing and the reduction of bead spreading and wettability. Alternatively, TM3 causes spattering, in which material is wasted and the working environment becomes untidy. The most serious effect is that the process becomes unstable, in terms of unexpected bead geometry and higher surface roughness. Also, the case study corroborates that the WAAM deposition process, especially the surface of the melt pool, is significantly sensitive to the wire position (Heralić et al., 2012). Either higher or lower the wire position can cause the transfer mode to change dramatically which impedes the quality of the deposition. From the perspective of data analysis and modelling, several features are extracted from arc voltage data which have shown a high relevance to the transfer mode, in terms of the values of variance, minimum, skewness and peak numbers in this research. Compared to other similar wire position research in WAAM, the proposed method discovers more features of the arc voltage in both time and frequency domains. Furthermore, by using a recurrent neural network, LSTM-NN, the hidden patterns become more obvious to spot compared to other conventional ML technologies.

It would be useful to find other features in the arc voltage which may improve the model accuracy in future work. Compared to other previous research regarding the process stability, this droplet transfer control approach can be easily implemented for different WAAM processing technologies, using for example different arc power sources which utilise and off axis wire feed method, and different materials, due to it is a data-driven approach. There is also potential for data

fusion of other process data sets such as process parameters, environmental conditions, plasma spectral analysis and deposition images. There are still some limitations of the case study. Firstly, the validation of the control system was mainly evaluated by the formation of spatters, wall geometry and the changing process between different droplet transfer modes. Other assessments such as variations in microstructure and mechanical properties of the deposited material parts dependent on to the droplet transfer mode could be evaluated. However, these effects are expected to be very small in comparison to other factors (Kobryn & Semiatin, 2003). Secondly, only oscillated walls and single-pass walls were built in the case study for evaluating the control system, which are two of the simplest shapes for WAAM production. More complex shapes and complete part manufacture will be used to evaluate the control system in future work. Finally, the study only evaluated the PTA based WAAM process with Ti-6Al-4V wire as the supply material. In future, it is this will extend to other WAAM systems, such as gas tungsten arc with other feed materials.

Conclusions

The purpose of this study was to develop an efficient and accurate model to determine the droplet transfer mode during the deposition process and dynamically adjust it to optimal status, to maintain the stability of the WAAM process through a droplet transfer control system. The approach was inspired by a review of relevant studies which indicate the significant importance of process stability and the state-of-the-art technologies of deep learning in the field of WAAM. Some highlights of this research are summarised as follows.

- Monitoring of the voltage on the feed wire in WAAM was found to be very suitable for the implementation of a droplet transfer control system
- Through the implementation of an ML algorithm a droplet transfer control system with a response time of about a second was enabled.
- It was demonstrated that this machine learning enabled control system is suitable for improving the process stability and consequent part quality in the production of simple structures by WAAM
- The LSTM-NN was found to be the most suitable ML algorithm compared to 3 conventional algorithms, *k*-NN, SVM and DT.

Acknowledgements The authors would like to thank NEWAM (EP/R027218/1) program for financial support. The authors also would like to thank Flemming Nielsen, Nisar Shah and John Thrower for the technical support.

Declarations

Conflict of interest The authors declare that they have no known competing financial interests or personal relationships that could have appeared to influence the work reported in this paper.

Open Access This article is licensed under a Creative Commons Attribution 4.0 International License, which permits use, sharing, adaptation, distribution and reproduction in any medium or format, as long as you give appropriate credit to the original author(s) and the source, provide a link to the Creative Commons licence, and indicate if changes were made. The images or other third party material in this article are included in the article's Creative Commons licence, unless indicated otherwise in a credit line to the material. If material is not included in the article's Creative Commons licence and your intended use is not permitted by statutory regulation or exceeds the permitted use, you will need to obtain permission directly from the copyright holder. To view a copy of this licence, visit <http://creativecommons.org/licenses/by/4.0/>.

References

- Abandah, G. A., Graves, A., Al-Shagoor, B., Arabiyat, A., Jamour, F., & Al-Tae, M. (2015). Automatic diacritization of Arabic text using recurrent neural networks. *International Journal on Document Analysis and Recognition (IJDAR)*, 18(2), 183–197. <https://doi.org/10.1007/s10032-015-0242-2>
- Andersen, K., Cook, G. E., Karsai, G., & Ramaswamy, K. (1990). Artificial neural networks applied to arc welding process modeling and control. *IEEE Transactions on Industry Applications*, 26(5), 824–830. <https://doi.org/10.1109/ias.1989.96968>
- Asuero, A. G., Sayago, A., & González, A. G. (2006). The correlation coefficient: An overview. *Critical Reviews in Analytical Chemistry*, 36(1), 41–59. <https://doi.org/10.1080/10408340500526766>
- Bonaccorso, G. (2017). *Machine learning algorithms*. Packt Publishing Ltd.
- Charaniya, S., Le, H., Rangwala, H., Mills, K., Johnson, K., Karypis, G., & Hu, W. S. (2010). Mining manufacturing data for discovery of high productivity process characteristics. *Journal of Biotechnology*, 147(3–4), 186–197. <https://doi.org/10.1016/j.jbiotec.2010.04.005>
- Cunningham, C. R., Flynn, J. M., Shokrani, A., Dhokia, V., & Newman, S. T. (2018). Invited review article: Strategies and processes for high quality wire arc additive manufacturing. *Additive Manufacturing*, 22, 672–686. <https://doi.org/10.1016/j.addma.2018.06.020>
- Desai, N., Dharmeliya, K., & Desai, V. (2013). Feature extraction and classification techniques for speech recognition: A review. *International Journal of Emerging Technology and Advanced Engineering*, 3(12), 367–371.
- Dilthey, U., Fuest, D., & Scheller, W. (1995). Laser welding with filler wire. *Optical and Quantum Electronics*, 27(12), 1181–1191.
- Ding, J., Colegrove, P., Martina, F., Williams, S., Wiktorowicz, R., & Palt, M. R. (2015). Development of a laminar flow local shielding device for wire+arc additive manufacture. *Journal of Materials Processing Technology*, 226, 99–105. <https://doi.org/10.1016/j.jmatprotec.2015.07.005>
- Fu, T. C. (2011). A review on time series data mining. *Engineering Applications of Artificial Intelligence*, 24(1), 164–181. <https://doi.org/10.1016/j.engappai.2010.09.007>
- Gulli, A., & Pal, S. (2017). *Deep learning with Keras*. Packt Publishing Ltd.
- Hagqvist, P., Heralić, A., Christiansson, A.-K., & Lennartson, B. (2014). Resistance measurements for control of laser metal wire deposition. *Optics and Lasers in Engineering*, 54, 62–67. <https://doi.org/10.1016/j.optlaseng.2013.10.010>
- Hagqvist, P., Heralić, A., Christiansson, A.-K., & Lennartson, B. (2015). Resistance based iterative learning control of additive manufacturing with wire. *Mechatronics*, 31, 116–123. <https://doi.org/10.1016/j.mechatronics.2015.03.008>
- Heralić, A., Christiansson, A. K., & Lennartson, B. (2012). Height control of laser metal-wire deposition based on iterative learning control and 3D scanning. *Optics and Lasers in Engineering*, 50(9), 1230–1241. <https://doi.org/10.1016/j.optlaseng.2012.03.016>
- Hossin, M., & Sulaiman, M. N. (2015). A review on evaluation metrics for data classification evaluations. *International Journal of Data Mining & Knowledge Management Process*, 5(2), 1–11. <https://doi.org/10.5121/ijdkp.2015.5201>
- Imanaga, S., Haneda, M., Shibata, N., Kobayashi, M., & Hino, E. (2000). Development of torch position control and welding condition control technology for all-position, multi-layer GTA welding. Development of fully automatic GTA welding system for pipes (2nd Report). *Welding International*, 14(5), 356–364. <https://doi.org/10.1080/09507110009549194>
- Khanna, N., Zadafiya, K., Patel, T., Kaynak, Y., Rahman Rashid, R. A., & Vafadar, A. (2021). Review on machining of additively manufactured nickel and titanium alloys. *Journal of Materials Research and Technology*, 15, 3192–3221. <https://doi.org/10.1016/J.JMRT.2021.09.088>
- Kobryn, P. A., & Semiatin, S. L. (2003). Microstructure and texture evolution during solidification processing of Ti–6Al–4V. *Journal of Materials Processing Technology*, 135(2–3), 330–339. [https://doi.org/10.1016/S0924-0136\(02\)00865-8](https://doi.org/10.1016/S0924-0136(02)00865-8)
- Marchi, E., Ferroni, G., Eyben, F., Gabrielli, L., Squartini, S., & Schuller, B. (2014). Multi-resolution linear prediction based features for audio onset detection with bidirectional LSTM neural networks. In *2014 IEEE international conference on acoustics, speech and signal processing (ICASSP)* (pp. 2164–2168). IEEE.
- Martina, F., Mehnen, J., Williams, S. W., Colegrove, P., & Wang, F. (2012). Investigation of the benefits of plasma deposition for the additive layer manufacture of Ti–6Al–4V. *Journal of Materials Processing Technology*, 212(6), 1377–1386. <https://doi.org/10.1016/J.JMATPROTEC.2012.02.002>
- Miranda, R. M., Lopes, G., Quintino, L., Rodrigues, J. P., & Williams, S. (2008). Rapid prototyping with high power fiber lasers. *Materials & Design*, 29(10), 2072–2075. <https://doi.org/10.1016/j.matdes.2008.03.030>
- Oda, Y., Fudaba, H., Neubig, G., Hata, H., Sakti, S., Toda, T., & Nakamura, S. (2015). Learning to generate pseudo-code from source code using statistical machine translation. In *2015 30th IEEE/ACM international conference on automated software engineering (ASE)* (pp. 574–584). IEEE.
- Pedregosa, F., Varoquaux, G., Gramfort, A., Michel, V., Thirion, B., Grisel, O., et al. (2011). Scikit-learn: Machine learning in Python. *The Journal of Machine Learning Research*, 12, 2825–2830.
- Qin, J., Hu, F., Liu, Y., Witherell, P., Wang, C. C. L., Rosen, D. W., et al. (2022). Research and application of machine learning for additive manufacturing. *Additive Manufacturing*, 52, 102691. <https://doi.org/10.1016/J.ADDMA.2022.102691>
- Raubitzek, S., & Neubauer, T. (2021). A fractal interpolation approach to improve neural network predictions for difficult time series data. *Expert Systems with Applications*, 169, 114474. <https://doi.org/10.1016/j.eswa.2020.114474>
- Ríos, S., Colegrove, P. A., & Williams, S. W. (2019). Metal transfer modes in plasma Wire+ Arc additive manufacture. *Journal of Materials Processing Technology*, 264, 45–54. <https://doi.org/10.1016/j.jmatprotec.2018.08.043>

- Riza Alvy Syafi'i, M. H., Prasetyono, E., Khafidli, M. K., Anggrawan, D. O., & Tjahjono, A. (2018). Real time series DC arc fault detection based on fast Fourier transform. In *2018 International electronics symposium on engineering technology and applications (IES-ETA)* (pp. 25–30). <https://doi.org/10.1109/ELECSYM.2018.8615525>
- Sherstinsky, A. (2020). Fundamentals of recurrent neural network (RNN) and long short-term memory (LSTM) network. *Physica d: Nonlinear Phenomena*, *404*, 132306. <https://doi.org/10.1016/J.PHYSD.2019.132306>
- Shi, M., Xiong, J., Zhang, G., & Zheng, S. (2021). Monitoring process stability in GTA additive manufacturing based on vision sensing of arc length. *Measurement*, *185*, 110001. <https://doi.org/10.1016/j.measurement.2021.110001>
- Sorensen, C. D., & Eagar, T. W. (1990). Measurement of oscillations in partially penetrated weld pools through spectral analysis, 463–468. <https://doi.org/10.1115/1.2896165>
- Wang, C., Suder, W., Ding, J., & Williams, S. (2021a). Wire based plasma arc and laser hybrid additive manufacture of Ti-6Al-4V. *Journal of Materials Processing Technology*, *293*, 117080. <https://doi.org/10.1016/j.jmatprotec.2021.117080>
- Wang, C., Suder, W., Ding, J., & Williams, S. (2021b). The effect of wire size on high deposition rate wire and plasma arc additive manufacture of Ti-6Al-4V. *Journal of Materials Processing Technology*, *288*, 116842. <https://doi.org/10.1016/J.JMATPROTEC.2020.116842>
- Wiens, T. S., Dale, B. C., Boyce, M. S., & Kershaw, G. P. (2008). Three way k-fold cross-validation of resource selection functions. *Ecological Modelling*, *212*(3–4), 244–255. <https://doi.org/10.1016/j.ecolmodel.2007.10.005>
- Williams, S. W., Martina, F., Addison, A. C., Ding, J., Pardal, G., & Colegrove, P. (2016). Wire+ arc additive manufacturing. *Materials Science and Technology*, *32*(7), 641–647. <https://doi.org/10.1179/1743284715Y.0000000073>
- Wu, B., Pan, Z., Ding, D., Cuiuri, D., Li, H., Xu, J., & Norrish, J. (2018). A review of the wire arc additive manufacturing of metals: Properties, defects and quality improvement. *Journal of Manufacturing Processes*, *35*, 127–139. <https://doi.org/10.1016/j.jmapro.2018.08.001>
- Xia, C., Pan, Z., Polden, J., Li, H., Xu, Y., Chen, S., & Zhang, Y. (2020). A review on wire arc additive manufacturing: Monitoring, control and a framework of automated system. *Journal of Manufacturing Systems*, *57*, 31–45. <https://doi.org/10.1016/j.jmsy.2020.08.008>
- Yudodibroto, B. Y. B., Hermans, M. J. M., Hirata, Y., & den Ouden, G. (2004). Influence of filler wire addition on weld pool oscillation during gas tungsten arc welding. *Science and Technology of Welding and Joining*, *9*(2), 163–168. <https://doi.org/10.1179/136217104225012274>
- Yue-Hei Ng, J., Hausknecht, M., Vijayanarasimhan, S., Vinyals, O., Monga, R., & Toderici, G. (2015). Beyond short snippets: Deep networks for video classification. In *Proceedings of the IEEE conference on computer vision and pattern recognition* (pp. 4694–4702)

Publisher's Note Springer Nature remains neutral with regard to jurisdictional claims in published maps and institutional affiliations.